

Chapter 2

Core concepts of microwave and RF measurements

2.1 Introduction

In this chapter we review the core concepts of microwave and radio frequency (RF) propagation in both guided-wave and on-wafer environments. Because most of these concepts are well-known, we will introduce only the terms and definitions that are necessary for the development and description of the material used throughout this book. For many, this chapter will serve as a whirlwind tour of familiar concepts. Readers interested in further details will find them in the referenced literature.

Guided waves are often discussed exclusively in terms of transmission line theory. Here, our approach will begin with Maxwell's equations, from which we will then transition to the transmission line approach. Readers who do not require a review of the fundamental physics of guided electromagnetic waves may wish to skip directly to Section 2.3, which provides an overview of transmission line theory. Building upon transmission line theory, we define the impedance, admittance and scattering parameter matrices. Then, after a brief discussion of signal flow graphs, we discuss calibration and de-embedding. From there, the calibration approach is extended to multimode propagation. Finally, we introduce one-port calibration of scanning microwave microscopes.

2.2 Maxwell's equations

2.2.1 Macroscopic equations

Without derivation, we define Maxwell's equations as follows:

$$\nabla \times \mathbf{E} = -\frac{\partial \mathbf{B}}{\partial t} \quad (2.1)$$

$$\nabla \times \mathbf{H} = \mathbf{J} + \frac{\partial \mathbf{D}}{\partial t} \quad (2.2)$$

$$\nabla \cdot \mathbf{D} = \rho \quad (2.3)$$

$$\nabla \cdot \mathbf{B} = 0 \quad (2.4)$$

where \mathbf{E} and \mathbf{H} are the electric and magnetic field vectors, respectively. \mathbf{B} and \mathbf{D} are the magnetic induction and electric displacement vectors, respectively. \mathbf{J} is a vector that represents the induced and enforced current densities and ρ is the charge density. \mathbf{E} , \mathbf{H} , \mathbf{B} , \mathbf{D} , \mathbf{J} and ρ are functions of position $\mathbf{r} = (x, y, z)$ and time t [1].

Maxwell's equations are complemented by the general electromagnetic materials equations:

$$\mathbf{B} = [\boldsymbol{\mu}] \cdot \mathbf{H} \quad (2.5)$$

$$\mathbf{D} = [\boldsymbol{\varepsilon}] \cdot \mathbf{E} \quad (2.6)$$

$$\mathbf{J} = [\boldsymbol{\sigma}] \cdot (\mathbf{E} + \mathbf{E}_{enf}) \quad (2.7)$$

where $[\boldsymbol{\mu}]$, $[\boldsymbol{\varepsilon}]$, $[\boldsymbol{\sigma}]$ are the permeability, permittivity and conductivity tensors, respectively. For isotropic media, these tensors are reduced to scalar quantities. Here, we will discuss propagation of electromagnetic waves only in media that are linear, isotropic and passive, unless otherwise specified. In addition to Maxwell's equations, one must enforce the continuity equation

$$\frac{\partial \rho}{\partial t} + \nabla \cdot \mathbf{J} = 0 \quad . \quad (2.8)$$

Finally, the particular solution of a given electromagnetic problem will depend on the boundary conditions at the interface between two different materials, denoted below by subscripts 1 and 2. For tangential components of electric and magnetic fields [1]

$$E_{t1} = E_{t2} \quad (2.9a)$$

$$H_{t1} = H_{t2} + K_s \quad , \quad (2.9b)$$

where K_s is the surface current density in A/m. For the normal components of the displacement and magnetic induction

$$B_{n1} = B_{n2} \quad (2.10a)$$

$$D_{n1} = D_{n2} - \rho_s \quad , \quad (2.10b)$$

where ρ_s is surface charge density in C/m².

2.2.2 Vector and scalar potentials

To gain physical insight into the meaning of Maxwell's equation within a material, it is necessary to introduce the polarization vector \mathbf{P} and magnetization vector \mathbf{M} as [2]

$$\mathbf{D} = \varepsilon_0 \mathbf{E} + \mathbf{P} \quad (2.11)$$

and

$$\mathbf{B} = \mu_0 (\mathbf{H} + \mathbf{M}) \quad . \quad (2.12)$$

Then the Equations (2.2) and (2.3) can be rewritten in the form:

$$\nabla \times \mathbf{B} = \mu_0 \mathbf{J} + \frac{1}{c^2} \frac{\partial \mathbf{E}}{\partial t} + \mu_0 \nabla \times \mathbf{M} + \mu_0 \frac{\partial \mathbf{P}}{\partial t} \quad (2.13)$$

$$\nabla \cdot \mathbf{E} = \frac{1}{\epsilon_0} (\rho + \nabla \cdot \mathbf{P}) \quad , \quad (2.14)$$

where c is speed of light in vacuum, ϵ_0 is the permittivity of free space, and μ_0 is the permeability of free space. Equations (2.1) and (2.4) retain their form. The material-related terms in Equation (2.13) represent the effective currents due to presence of the material and in Equation (2.14) the bound charge due to presence of the material. We will discuss polarization and magnetization vectors and their relation to microscopic material parameters in Chapter 9.

From Equation (2.4), it follows that the magnetic field can be written in the form

$$\mathbf{B} = \nabla \times \mathbf{A} \quad . \quad (2.15)$$

The vector field \mathbf{A} is known as the vector potential. Combining this definition with Equation (2.1), we can define a scalar quantity ϕ called the scalar potential such that the electric field can be expressed as

$$\mathbf{E} = -\frac{\partial \mathbf{A}}{\partial t} - \nabla \phi \quad . \quad (2.16)$$

Note that \mathbf{A} and ϕ are both functions of \mathbf{r} and t . This form of Maxwell's equations is indispensable for describing nanoscale electromagnetic interactions with matter. The introduction of potentials in (2.15) and (2.16) does not uniquely determine \mathbf{A} and ϕ . By introducing the so called Lorentz gauge condition

$$\nabla \cdot \mathbf{A} + \frac{1}{c^2} \frac{\partial \phi}{\partial t} = 0 \quad , \quad (2.17)$$

\mathbf{A} and ϕ can be uniquely determined from

$$(\nabla^2 - \frac{\partial^2}{\partial t^2})\mathbf{A} = -\mu_0 \mathbf{J} \quad (2.18)$$

and

$$(\nabla^2 - \frac{\partial^2}{\partial t^2})\phi = -\frac{1}{\epsilon_0} \rho \quad . \quad (2.19)$$

The general solutions for the scalar and vector potentials in the Lorentz gauge have the following respective forms [3]-[5]:

$$\varphi(\mathbf{r}, t) = \left[\frac{1}{4\pi\epsilon_0} \int_{-\infty}^{\infty} \frac{\rho(\mathbf{r}', t - \frac{|\mathbf{r}-\mathbf{r}'|}{c})}{|\mathbf{r}-\mathbf{r}'|} d^3\mathbf{r}' \right] \quad (2.20)$$

and

$$\mathbf{A}(\mathbf{r}, t) = \left[\frac{\mu_0}{4\pi} \int_{-\infty}^{\infty} \frac{J(\mathbf{r}', t - \frac{|\mathbf{r} - \mathbf{r}'|}{c})}{|\mathbf{r} - \mathbf{r}'|} d^3\mathbf{r}' \right] . \quad (2.21)$$

These potentials are sometimes referred to as retarded potentials. Note the presence of the expression for the so-called retarded time, $t - |\mathbf{r} - \mathbf{r}'|/c$. Also note that the current densities and charge densities in these equations are assumed to contain all contributions including sources. We will return to this approach and its consequences when we discuss near-field interactions.

2.2.3 Hertz vector potentials

In order to solve Maxwell's equations in guided waves systems, it is useful to introduce the Hertz potential $\boldsymbol{\pi}$ that is related to the vector and scalar potentials through [6]

$$\mathbf{A}(\mathbf{r}, t) = \varepsilon\mu \frac{\partial \boldsymbol{\pi}(\mathbf{r}, t)}{\partial t}. \quad (2.22)$$

Using the Lorentz gauge condition (2.17)

$$\varphi(\mathbf{r}, t) = -\nabla \cdot \boldsymbol{\pi} \quad (2.23)$$

Note that if one can find an arbitrary solution for $\boldsymbol{\pi}$, the electric and magnetic fields obtained from the Hertz vector fulfill all of Maxwell's equations and therefore describe the solution of the problem.

Inspection of Maxwell's equations for guided waves propagating in the z direction reveals two special solutions: one when $E_z = 0$ and the other when $H_z = 0$, where E_z and H_z are the components of the electric and magnetic fields along the direction of propagation. The first of these solutions has the electric field perpendicular to the direction of propagation and is called the transverse electric (TE) mode. The latter of these solutions has the magnetic field perpendicular to the direction of propagation and is called the transverse magnetic (TM) mode. The solution for these two cases simplifies if we introduce special forms of Hertz vector potentials: the electric Hertz vector potential $\boldsymbol{\pi}_e$ and magnetic Hertz vector potential $\boldsymbol{\pi}_m$. Below, we introduce formulas that correspond to propagation of guided waves in the positive z direction. For the propagation in the negative z direction they have to be modified appropriately [7]. The electric Hertz vector is defined such that:

$$\mathbf{E} = \nabla \times \nabla \times \boldsymbol{\pi}_e \quad , \quad (2.24a)$$

$$\mathbf{H} = \epsilon \frac{\partial}{\partial t} (\nabla \times \boldsymbol{\pi}_e) \quad . \quad (2.24b)$$

The magnetic Hertz vector is defined as:

$$\mathbf{H} = \nabla \times \nabla \times \boldsymbol{\pi}_m \quad , \quad (2.25a)$$

$$\mathbf{E} = -\mu \frac{\partial}{\partial t} (\nabla \times \boldsymbol{\pi}_m) \quad . \quad (2.25b)$$

Both vectors satisfy the wave equation

$$\nabla^2 \boldsymbol{\pi}_{e,m} - \mu \varepsilon \frac{\partial^2}{\partial t^2} (\boldsymbol{\pi}_{e,m}) = 0 \quad . \quad (2.26)$$

When the time dependence of the electric and magnetic fields is harmonic, i.e. in the form $\exp(j\omega t)$, one can replace $\frac{\partial}{\partial t}$ by $j\omega$, where ω is the radial frequency of the harmonic signal and $j = \sqrt{-1}$.

The solution of (2.26), as mentioned above, defines all components of guided-wave electromagnetic fields through (2.24) and (2.25). The utility of the Hertz vector is demonstrated by the fact that one can easily obtain the transverse component of the magnetic field, the so-called TM field, from the component of the electric Hertz vector in the direction of propagation. In a similar way, one can easily obtain the transverse component of the electric field, the so-called TE field, from the magnetic Hertz vector.

If the propagating electromagnetic field has both electric and magnetic field components in the plane perpendicular to the direction of propagation and these fields are a function of only one coordinate variable and time, then this field configuration is called a transverse electromagnetic or TEM wave. TEM waves play an important role in microwave engineering because the form of propagating TEM wave equations is similar to that transmission line equations, as will be shown below.

2.2.4 Transition from fields to transmission lines

Following the approach presented in [7], we transition from the electromagnetic field representation to the quasi-equivalent transmission line approach. The transmission line model is widely used as it represents complex electromagnetic fields through conceptually simpler voltages and currents. Here, the case of TE waves is described in detail, but the approach is also valid for TM and TEM waves.

Assuming the propagation direction is in the z direction for TE waves, the $\boldsymbol{\pi}_m$ vector can be expressed as:

$$\boldsymbol{\pi}_m = T_e(x, y)L(z)\mathbf{u}_z, \quad , \quad (2.27)$$

where \mathbf{u}_z a unit vector in the z direction and the functions T_e and L represent the transverse and longitudinal field components, respectively. Inserting (2.27) into (2.26) and separating the variables, we get two differential equations

$$\nabla^2 T_e(x, y) + K^2 T_e(x, y) = 0 \quad , \quad (2.28a)$$

$$\frac{d^2 L(z)}{dz^2} + \gamma^2 L(z) = 0 \quad , \quad (2.28b)$$

where $\gamma^2 = \varepsilon\mu - K^2$ and K is the separation constant. The solution of (2.28b) is in the form

$$L(z) = Ae^{-\gamma z} + Be^{\gamma z}, \quad (2.29)$$

which represents the wave propagation as a superposition of waves propagating in the positive and negative z directions. The propagation constant is a complex number, $\gamma = \alpha + j\beta$, where α is the damping parameter and β is a phase constant. One subsequently can introduce $\lambda_g = \frac{2\pi}{\beta}$, the wavelength of the guided-wave mode. Both Equations (2.28a) and (2.28b) have to be solved as eigenvalue problems with corresponding boundary conditions. We are not going to address the mathematical solution of such eigenvalue problems here. In general, the solution of the boundary value problem for TE and TM modes leads to an infinite number of solutions for each of the modes. The existence of this set of solutions and the guided wave mode structure it represents are critical concepts for the understanding of guided waves.

Now we define the circuit variables for voltage v and current i in terms of the guided-wave electromagnetic fields. The transverse magnetic and electric components of are defined as

$$\mathbf{H}_t = i\mathbf{h}^0, \quad (2.30a)$$

$$\mathbf{E}_t = v\mathbf{e}^0. \quad (2.30b)$$

For the TE mode:

$$\mathbf{h}^0 = C_2 \nabla T_e, \quad (2.31a)$$

$$\mathbf{e}^0 = C_1 (\mathbf{u}_z \times \nabla T_e), \quad (2.31b)$$

and for the TM mode:

$$\mathbf{h}^0 = j\omega\varepsilon C_2 (\nabla T_m \times \mathbf{u}_z), \quad (2.32a)$$

$$\mathbf{e}^0 = C_1 \nabla T_m. \quad (2.32b)$$

C_1 and C_2 are constants. Combining Equation (2.32) with Equations (2.26) through (2.29) and assuming harmonic time dependence one gets

$$v = \frac{j\omega\mu L(z)}{C_1}, \quad (2.33a)$$

$$i = \frac{dL(z)/dz}{C_2}. \quad (2.33b)$$

Note that v and i represent the voltages and currents of the particular propagating mode under specified boundary conditions. It is assumed that the product ($v \cdot i^*$) is

proportional to power flow of the mode and the ratio $\frac{v}{i} = Z$ is the impedance of the mode. We can define the power in the usual way for electric circuits as $P = \frac{1}{2} \text{Re}(v \cdot i^*)$. This definition of the power imposes the condition that only one of the constants C_1 and C_2 is arbitrary. The arbitrary constant is obtained from additional requirements representing normalization conditions, which are usually chosen such that the fields do not contradict basic physics. In the case of lines such as coaxial cables that have a principal mode, the transverse electric field obeys the Laplace equation. Therefore, one can integrate along the path between the electrodes to obtain the voltage between them. This defines uniquely the outstanding, arbitrary constant. The interested reader can find further details in References [2], [5], and [7] – [11].

With i and v defined, we can now define the characteristic impedance of the mode. Begin with the following relation between the transverse field components

$$\mathbf{u}_z \times \mathbf{H}_t = \mathbf{u}_z \times iC_2 \nabla T_e = \frac{iC_2}{vC_1} \mathbf{E}_t = \frac{C_2}{C_1 Z} \mathbf{E}_t \quad . \quad (2.34)$$

For a TE mode propagating in air, it can be shown that

$$\frac{C_1}{C_2} Z = Z_{0TE} = \left(\frac{\mu_0}{\epsilon_0}\right)^{1/2} \frac{\lambda_g}{\lambda_0} \quad , \quad (2.35)$$

where Z_{0TE} is the characteristic impedance of the TE mode, and λ_0 is the free space wavelength. The characteristic impedance of the TM mode can be found in a similar way [12]

$$Z_{0TM} = \left(\frac{\mu_0}{\epsilon_0}\right)^{1/2} \frac{\lambda_0}{\lambda_g} \quad . \quad (2.36)$$

Note that this definition of the characteristic impedance is not unique. It is not possible to uniquely define the characteristic impedance of the guided wave in general, but this definition is a reasonable one.

Finally, for completeness, it necessary to describe power flow in a guided-wave configuration. For electromagnetic fields the power flow is represented by Poynting's vector

$$\mathbf{S} = \mathbf{E} \times \mathbf{H} \quad . \quad (2.37)$$

In a guided-wave structure, the power flow is obtained by integrating the normal component of the Poynting vector over the waveguide cross section. Up to now, we used a general approach that depends on the solution of a boundary value problem of arbitrary configuration. It has allowed us to introduce the concepts of currents and voltages in a general sense for the transverse components of an arbitrary guided-wave field configuration, paving the way for the introduction of transmission line theory.

2.3 Transmission line theory

Although the theory of guided electromagnetic waves can be fully developed from Maxwell's equations, the concepts of electrical circuits, including both lumped-element and distributed circuits, are widely used in microwave engineering. If the electromagnetic problem can be reduced to the propagation of a TEM wave, the circuit representation provides utility and fundamental insight. TEM-like waves are the principal modes of widely-used waveguides such as coaxial cables, microstrip lines, and coplanar waveguides. Here we will use the framework of circuit theory to introduce transmission line theory along with many key terms and concepts used throughout this book.

We will follow an approach introduced in the early stages of the development of microwave electronics [12]. Transmission line theory was originally developed by Heaviside [13] and the interested reader can find further details in a number of texts [14] – [17]. Having introduced current i and voltage v , propagation of a TEM mode in one direction is reduced to the propagation of a voltage or current wave on a transmission line of a finite length l . Note that in the context of microwave metrology, the transmission line concept is advantageous over pure circuit theory as it allows for easier definition of measurement reference planes.

Figure 2.1. **Transmission line model.** A schematic of a segment of a transmission line. The line of infinitesimal length dz is characterized by per-unit-length electrical circuit elements: resistance R_0 , inductance L_0 , capacitance C_0 and conductance G_0 .

A transmission line is characterized by per-unit-length electrical circuit elements: resistance R_0 , inductance L_0 , capacitance C_0 and conductance G_0 as shown in Fig. 2.1. These parameters depend on transmission line dimensions and the materials used to construct the line. Applying Kirchoff's laws for this infinitesimally long element yields the Telegrapher's equations:

$$\frac{dV(z)}{dz} = -(R_0 + j\omega L_0)I(z) \quad , \quad (2.38a)$$

$$\frac{dI(z)}{dz} = -(R_0 + j\omega L_0)V(z) \quad . \quad (2.38b)$$

We use the capital italicized letters I and V to represent the current i and voltage v with assumed harmonic time dependence. Taking the expression for $I(z)$ from (2.38b) and inserting into (2.38a) gives the wave equation for voltage. The wave equation for current can be obtained in a similar way. The solution of this wave equation is in the form (2.29), but with $L(z)$ replaced by voltage $V(z)$:

$$V(z) = V_+ e^{-\gamma z} + V_- e^{\gamma z} \quad . \quad (2.39)$$

As in (2.29), the solution is a superposition of forward-propagating wave (from the source) and backward-propagating wave (from the load). Unique values of V_+ and V_-

are obtained from the voltage and current and the load impedance at the end of the transmission line. If the transmission line of length l is terminated by a load impedance Z_L and we move the origin of the coordinate system there, then the expression $V_+e^{-\gamma l}$ represents the voltage wave incident on the load and $V_-e^{\gamma l}$ represents the voltage wave propagating away from this load.

The propagation constant and characteristic impedance of the transmission line are functions of the per-unit-length circuit elements:

$$\gamma = [(R_0 + j\omega L_0) \cdot (G_0 + j\omega C_0)]^{1/2} \quad (2.40)$$

and

$$Z_0 = \sqrt{\frac{(R_0 + j\omega L_0)}{(G_0 + j\omega C_0)}} \quad , \quad (2.41)$$

respectively. From (2.38a) and (2.39), the current is

$$I(z) = \frac{\gamma}{(R_0 + j\omega L_0)} (V_+e^{-\gamma z} - V_-e^{\gamma z}) = \frac{1}{Z_0} (V_+e^{-\gamma z} - V_-e^{\gamma z}) \quad . \quad (2.42)$$

We assume that the voltage (V_2) and current (I_2) at the load are known and define them as

$$V_2 = Z_L I_2 \quad , \quad (2.43)$$

where Z_L is the load impedance. The boundary conditions for obtaining the amplitudes of the forward and backward waves become

$$V(l) = V_2 = V^+ e^{-\gamma l} + V^- e^{\gamma l} \quad (2.44)$$

and

$$I(l) = I_2 = \frac{1}{Z_0} (V^+ e^{-\gamma l} - V^- e^{\gamma l}) \quad . \quad (2.45)$$

The solution of these two equations for V^+ and V^- gives

$$V^+ = \frac{1}{2} (V_2 + Z_0 I_2) e^{\gamma l} = V_+ e^{\gamma l} \quad , \quad (2.46a)$$

$$V^- = \frac{1}{2} (V_2 - Z_0 I_2) e^{-\gamma l} = V_- e^{-\gamma l} \quad . \quad (2.46b)$$

Inserting (2.46) into (2.39) and (2.42) and rearranging terms yields

$$V(z) = \frac{V_2 + Z_0 I_2}{2} e^{\gamma(l-z)} + \frac{V_2 - Z_0 I_2}{2} e^{-\gamma(l-z)} = V_{FW}(z) + V_{BW}(z) = V_2 \cosh \gamma(l-z) + Z_0 I_2 \sinh \gamma(l-z) \quad (2.47)$$

and

$$I(z) = \frac{V_2 + Z_0 I_2}{2Z_0} e^{\gamma(l-z)} - \frac{V_2 - Z_0 I_2}{2Z_0} e^{-\gamma(l-z)} = I_{FW}(z) - I_{BW}(z) = I_2 \cosh(l-z) - \frac{V_2}{Z_0} \sinh \gamma(l-z) \quad (2.48)$$

Equations (2.47) and (2.48) give the forward and backward propagating voltage and current waves – V_{FW} , V_{BW} , I_{FW} , and I_{BW} – as functions of V_2 and I_2 .

In practice, it is useful to know the ratio of the backward propagating wave to the forward propagating wave. This ratio reveals what fraction of the wave is reflected backward as a function of the load impedance or other inhomogeneity in the transmission line. This ratio is called reflection coefficient Γ and it can be expressed at any position z along the transmission line as

$$\Gamma(z) = \frac{V_{BW}}{V_{FW}} = \frac{V_2 - Z_0 I_2}{V_2 + Z_0 I_2} e^{-2\gamma(l-z)} = \frac{Z_L - Z_0}{Z_L + Z_0} e^{-\gamma(l-z)} \quad (2.49)$$

The impedance Z at any position along the transmission line is given by

$$Z(z) = \frac{V(z)}{I(z)} = Z_0 \frac{(Z_L + Z_0)e^{\gamma(l-z)} + (Z_L - Z_0)e^{-\gamma(l-z)}}{(Z_L + Z_0)e^{\gamma(l-z)} - (Z_L - Z_0)e^{-\gamma(l-z)}} = Z_0 \frac{1 + \Gamma(z)}{1 - \Gamma(z)} \quad (2.50)$$

Evaluating Equation (2.49) at the position $z = l$ yields:

$$\Gamma = \frac{Z_L - Z_0}{Z_L + Z_0} \quad (2.51)$$

This equation can be graphically represented by use of a Smith chart (or Smith diagram). The Smith chart visualizes the magnitude and phase of the reflection coefficient as a function of the load impedance. More generally, the Smith chart may be used to plot the reflection coefficient as a function of position along a transmission line or as a function of frequency. Several simple examples of impedance values are graphed on a Smith chart in Fig. 2.2. The radius of the chart is equal to one, representing full reflection of an incident signal. Thus, the position corresponding to an open circuit lies on the real axis with a value equal to positive one. The reflection coefficient of a short circuit is 180 degrees out of phase from the open-circuit reflection and therefore its position on the Smith chart is also on the real axis, but with a value equal to negative one. For an impedance-matched load, the reflection coefficient is equal to zero and therefore the position of the matched impedance in the Smith chart is at the center. Usually the reflection coefficient is frequency- and position-dependent. Therefore, the impedance change along the transmission line at a given fixed frequency may be represented by a parametric curve with distance from the beginning or end of the transmission line as a parameter. Likewise, for a fixed position on a transmission line, the frequency dependence of the impedance may be represented by a similar curve.

Figure 2.2. **The Smith chart.** The positions of several possible loads are shown: an open circuit, a short circuit and a matched load Z_0 . Examples of a constant resistance curve and a constant reactance curve are shown in gray.

Finally, an understanding of the power transmitted through a transmission line is of fundamental importance because it allows a unique definition of the relationship between the currents and voltages on the transmission line. Under the assumption of harmonic time dependence, the power transmitted through the cross section of a transmission line at position $z = z_1$ along the transmission line is

$$P_W = \frac{1}{2} \text{Re}(V(z_1)I^*(z_1)) \quad , \quad (2.52)$$

where the asterisk denotes the complex conjugate. Using the previously introduced forward and backward waves this can be rewritten as

$$P_W = \frac{1}{2} \text{Re}\{V_{FW}(z_1)I_{FW}^*(z_1) - V_{BW}(z_1)I_{BW}^*(z_1) + (V_{BW}(z_1)I_{FW}^*(z_1) - V_{FW}(z_1)I_{BW}^*(z_1))\} . \quad (2.53)$$

It follows that the power transmitted through a transmission line is not simply the difference of the power transmitted by the forward and backward waves, but also includes the interaction of these waves on the transmission line. This result is not surprising since the superposition principle applies only to voltages and currents (in linear circuits), but not to power.

2.4 Impedance, admittance and scattering matrixes

From basic circuit theory one can write equations that describe the relationships between the voltages and currents at each port of a multiport device. In order to calibrate and analyze the microwave measurements it is useful to describe these relationships in terms of impedance, admittance, and scattering parameters. Here, we will develop this approach for a two port configuration, but the approach can be generalized to any number of ports. Following convention, we introduce the currents at port 1 (I_1) and port 2 (I_2) and the corresponding voltages (V_1 and V_2) as shown in Fig. 2.3. If the network is linear, then the voltages will be linear functions of currents:

$$V_1 = Z_{11}I_1 + Z_{12}I_2 \quad , \quad (2.54a)$$

$$V_2 = Z_{21}I_1 + Z_{22}I_2 \quad , \quad (2.54b)$$

where the variables Z_{ij} have the units of impedance and collectively form an impedance matrix. From the reciprocity principle for passive linear circuits, it follows that $Z_{12} = Z_{21}$. Alternative representations may be developed by choosing variables other than V_1 and V_2 to be the dependent independent variables. For example, equations could be written for I_1 and I_2 as functions of V_1 and V_2 with the matrix of corresponding coefficients representing admittances. As yet another alternative, the so-called “h-

matrix representation,” equations could be written with the input voltage and the output current as the dependent variables.

Figure 2.3. **A two-port device.** A schematic of a two-port device defines the currents (I_1 and I_2), voltages (V_1 and V_2), and power waves (a_1, a_2, b_1, b_2).

At microwave frequencies, it is extremely difficult to directly measure voltages and currents. Therefore, a different approach had to be introduced that is more suitable for metrology at these frequencies. Assume that a two-port device is inserted (embedded) into a transmission line. We will call this device the device under test or DUT. Recall from Equations (2.46) that the voltages and currents at a port can be expressed as a superposition of waves propagating toward and away from the port. Here, the amplitudes of the waves propagating towards and away from a given port n are V_{n+} and V_{n-} . We can express the amplitudes of the waves propagating away from the port as functions of the amplitudes of the waves propagating towards the port n . Specifically, for a linear, two-port DUT:

$$V_{1-} = S_{11}V_{1+} + S_{12}V_{2+} \quad , \quad (2.55a)$$

$$V_{2-} = S_{21}V_{1+} + S_{22}V_{2+} \quad . \quad (2.55b)$$

The coefficients S_{ij} are called scattering parameters and collectively form a scattering matrix. The scattering matrix relates the waves reflected or scattered from the network to those incident upon the network. The scattering matrix parameters are sometimes referred to as “S parameters.” In a two-port device, the physical meaning of S_{11} is the input reflection coefficient when the output is matched ($V_{2+} = 0$), S_{21} is the forward transmission from port 1 to port 2, S_{12} is the reverse transmission from port 2 to port 1, and S_{22} is the reflection coefficient at port 2. An $n \times n$ matrix for an n -port device is considered reciprocal when $S_{ij} = S_{ji}$ and symmetric if it is reciprocal and $S_{ii} = S_{jj}$ for all values of i and j .

In commercial test equipment such as vector network analyzers, the scattering matrix parameters are usually normalized following the procedure introduced in Reference [18], in which the waves are defined in terms of the complex amplitudes of the incident and reflected power waves. This was done to make their definition consistent with the conservation of energy. Voltage amplitudes, on the other hand, have to be normalized to an arbitrary reference impedance. Usually, the characteristic impedance of the line is used as the normalization constant. Note that the characteristic impedance for each port, Z_{0n} , can differ from port to port. By convention, the reference impedance is 50Ω for most commercial test equipment. The power waves have amplitudes a_n and b_n , which are related to the voltage amplitudes introduced in (2.46) as follows:

$$a_n = \frac{V_{n+} + Z_{0n}I_n}{2\sqrt{|Re(Z_{0n})|}} = \frac{V_{n+}}{\sqrt{|Re(Z_{0n})|}}; \quad (2.56a)$$

$$b_n = \frac{V_n - Z_{0n} I_n}{2\sqrt{|Re(Z_{0n})|}} = \frac{V_n -}{\sqrt{|Re(Z_{0n})|}} \quad . \quad (2.56b)$$

Note that the amplitudes have the dimension of square root of power. From these definitions, the relation between the port voltages and currents for port n and the power waves is:

$$V_n = \sqrt{|Re(Z_{0n})|} (a_n + b_n) \quad , \quad (2.57a)$$

$$I_n = \frac{1}{\sqrt{|Re(Z_{0n})|}} (a_n - b_n) \quad . \quad (2.57b)$$

A set of equations analogous to (2.55) expressed in terms of the two-port power waves a and b can be obtained:

$$b_1 = S_{11}a_1 + S_{12}a_2 \quad , \quad (2.58a)$$

$$b_2 = S_{21}a_1 + S_{22}a_2 \quad . \quad (2.58b)$$

In terms of the power waves, the incident power into port n is

$$P_n = \frac{1}{2} (a_n a_n^* - b_n b_n^*) \quad . \quad (2.59)$$

It is important to remember that the scattering matrix is well-defined only if all ports are matched, though Z_{0n} and thus the matching condition may generally vary from port to port. In practice, the scattering matrix formulation is convenient for measurements as well as simulations. Therefore, microwave network analyzers are designed to measure scattering parameters.

In order to perform meaningful, quantitative measurements, it is necessary to define reference planes. When a two-port DUT is embedded into a transmission line, one may define specific reference planes at the ports of the device. Sometimes it is not possible to measure the response of the DUT at these reference planes. In that case, one has to do measurements at different, accessible planes and then translate them to the ports of the DUT. Fortunately, the scattering matrix formulation is amenable to the translation of the reference planes within a DUT. If the distance between the new reference plane to port 1 of the device is l_1 and the distance to port 2 is l_2 then the relation between the scattering matrix measured at the reference plane S and the translated scattering matrix S' at the reference plane of the DUT are expressed as:

$$[S'] = \begin{bmatrix} e^{-\gamma_1 l_1} & 0 \\ 0 & e^{-\gamma_2 l_2} \end{bmatrix} [S] \begin{bmatrix} e^{-\gamma_1 l_1} & 0 \\ 0 & e^{-\gamma_2 l_2} \end{bmatrix} \quad . \quad (2.60)$$

Despite these advantages, there are applications where the S parameter representation is not optimal. For example, the scattering matrix representation is inconvenient for cascading multiple devices. Cascading of matrices is more easily

accomplished by converting the scattering matrix parameters to transfer matrix parameters T_{ij} :

$$\begin{bmatrix} b_1 \\ a_1 \end{bmatrix} = \begin{bmatrix} T_{11} & T_{12} \\ T_{21} & T_{22} \end{bmatrix} \cdot \begin{bmatrix} a_2 \\ b_2 \end{bmatrix} = \begin{bmatrix} S_{12} - \frac{S_{22}S_{11}}{S_{21}} & \frac{S_{11}}{S_{21}} \\ -\frac{S_{22}}{S_{21}} & \frac{1}{S_{21}} \end{bmatrix} \cdot \begin{bmatrix} a_2 \\ b_2 \end{bmatrix} \quad (2.61)$$

The transfer matrix parameters are sometimes referred to as “T parameters.” The Interested reader can find other useful matrix transformation in Reference [8].

2.5 Signal flow graphs

Sometimes, it is useful to represent a system of linear equations in a graphical form. In the context of RF and microwave calibration procedures, this approach is particularly useful for the development of error models and error corrections, as we will see below. Here, we briefly review the basic principles. The system of linear equations to be represented by this graphical approach has the general form [19], [20]

$$\mathbf{y} = [\mathbf{M}]\mathbf{x} + [\mathbf{M}']\mathbf{y} \quad (2.62)$$

where $[\mathbf{M}]$ and $[\mathbf{M}']$ are square matrices with n columns and rows, the vector \mathbf{x} represents the n independent variables and the vector \mathbf{y} the n dependent variables. This system of equations is quite general and can be applied to many systems, including circuits with closed signal loops. If there are no direct signal loops, Equation (2.62) simplifies to the standard scattering matrix Equations (2.55). A signal flow graph consists of a set of nodes that are connected by branches. Each pair of nodes represents the amplitudes of an incident and an exciting wave: an “ a ” and a “ b ”, as defined in (2.56). The branches represent the complex S parameters that relate the wave amplitudes. In other words, they represent the gains or losses along the path between two nodes. Note that the branches have a specified direction, denoted by an arrow, and that signals propagate only in the direction of arrows. For example, if a port is terminated by a load, then the corresponding pair of nodes is connected via an additional branch, with the load branch corresponding to the reflection coefficient of the load.

The transfer function of a signal flow graph may generally be determined by application of the so-called “Mason’s rules.” It is often helpful to simplify the graph by use of four simple rules that govern the algebra of signal flow graphs:

- 1) *Series rule*: Two sections in series can be reduced to one with the resulting gain given by multiplication of the two S parameters. (see Fig. 2.4(a))
- 2) *Parallel rule*: Two branches in parallel pointing into the same node can be replaced by one with the gain equal to the sum of the two S parameters, or, more generally, the S parameters of all branches entering a node may be summed. (see Fig. 2.4(b))

- 3) *Loop/self-loop rule*: Branches that begin and end at the same node are “self-loops.” A self-loop can be eliminated by multiplying all branches feeding the self-loop node by $1/(1 - S_{sl})$ where S_{sl} is the gain of the self-loop. (Fig. 2.4(c))
- 4) *Splitting rule*: If a node has exactly one incident branch and one or more exiting branches, the incoming branch can be “split” and directly combined with each of the exiting branches. This rule can be used to treat the loops (arrows in parallel branches point to different directions). (Fig. 2.4(d))

With experience, one can learn when it is most advantageous to use the signal flow graph approach and when it is more advantageous to use a matrix formulation.

Figure 2.4. **Rules for simplifying signal flow graphs.** (a) Series rule (b) Parallel rule (c) Loop / self-loop rule (d) Splitting rule.

2.6 Device de-embedding and calibration

2.6.1 De-embedding

A central topic of this book is the measurement of nanoscale devices at radio frequencies. Many nanoscale device measurements are implemented as one- or two-port scattering parameter measurements with a vector network analyzer (VNA). As a result, we will focus on de-embedding of devices, calibration techniques and simple error models for such measurements. Nanoscale devices are generally integrated with a larger test structure that includes host structures, probes, connectors, and contacts. We will refer to such blocks of elements external to the nanoscale DUT as test fixtures. VNA measurements are usually done at reference planes that includes both the fixture and the DUT, which we will refer to as the “coaxial reference plane,” as this reference plane often coincides with a coaxial connector. To be able to accurately characterize the DUT, one needs to remove the test fixture characteristics from the measurements.

Broadly speaking, there are many different approaches for removing the effects of the fixtures. Fundamentally, each of these approaches may be classified either as a “direct measurement” or as a “de-embedding”. In the first case there are two stages. First a series of measurements of are made with physical reference standards inserted into the fixture in place of the DUT. Subsequently direct measurement of the DUT is performed. The reference planes are positioned at the boundary of the fixture and DUT. This approach requires development of specialized physical reference standards. As a result, the precision of direct measurement results depends on the quality of these physical standards.

By contrast, a de-embedding procedure uses models of test fixtures. These models are either mathematical or obtained experimentally, especially in the case on-wafer measurements, which are discussed below. Using these models, we can analytically remove the fixtures from the measurement. The precision of this approach depends

once again on the accuracy of the model used. We will use both the direct measurement and de-embedding approaches throughout this book.

The concept of scattering parameters together with the flow graph approach is especially useful for the development of the theory of de-embedding fixtures from the measurements. Fig. 2.5 shows the signal flow graph for a two-port fixtured measurement with both the fixtures and the DUT represented by S parameters. The outer and inner pairs of dashed lines represent the coaxial and DUT reference planes, respectively. The properties of the two test fixtures are describe by the scattering parameter matrix elements $S^{FA_{ij}}$ and $S^{FB_{ij}}$.

Figure 2.5. A fixtured, two-port measurement. The properties of the DUT are represented by S parameter matrix elements S_{ij} . The properties of the two fixtures are represented by S parameter matrix elements $S^{FA_{ij}}$ and $S^{FB_{ij}}$. The four grey, dashed lines represent reference planes. The outer pair represent the coaxial reference planes while the inner pair represent DUT reference planes.

Matrix algebra provides the simplest approach to de-embed the scattering parameters of the DUT from the measurements. First, one needs to convert the S parameter matrices of the measurement, both test fixtures and the DUT to T-parameter matrices using (2.46). Then

$$\mathbf{T}^m = \mathbf{T}^{FA} \mathbf{T}^{DUT} \mathbf{T}^{FB} \quad , \quad (2.63)$$

where \mathbf{T}^m is the T matrix from the VNA measurements, and \mathbf{T}^{FA} , \mathbf{T}^{FB} , and \mathbf{T}^{DUT} are the T matrices for fixture A, fixture B, and the DUT, respectively. Multiplying by the inverse T matrices of fixtures yields

$$\mathbf{T}^{DUT} = [\mathbf{T}^{FA}]^{-1} \mathbf{T}^m [\mathbf{T}^{FB}]^{-1} \quad . \quad (2.64)$$

The S parameters of the device are then obtained by converting \mathbf{T}^{DUT} back to an S parameter matrix.

2.6.2 Multiline TRL and other calibration techniques

In general, there is no “ideal” measurement test equipment. Therefore, the measurement strategy is to evaluate deviations from ideal behavior and to remove these systematic deviations from the measurements through calibration, thus significantly improving the accuracy of network analyzer measurements. This in turn provides the most accurate picture of device performance.

Many approaches have been developed for calibrated scattering parameter measurements. Detailed descriptions of coaxial-plane calibration techniques can be found in manufacturers’ applications notes [21] – [23] as well as published papers [24] – [26]. Many of these approaches were initially developed for a coaxial environment, but have since been adapted to the on-wafer environment. In this book, considerable

use is made of the multiline thru-reflect-line (TRL) calibration procedure and therefore we will often focus on that approach. Multiline TRL offers a high degree of precision and utilizes an easily-implemented set of calibration standards, however many alternative calibration techniques exist. For example, the short-open-line-thru (SOLT) calibration, for example, utilizes symmetric open lines, symmetric shorted lines, a line of known length and a thru line that is short enough that one can assume that the transmission is unity. Another possibility is the line-reflect-match (LRM) calibration, which supplements the SOLT calibration with a symmetric 50 ohm load. There is one important limitation all these standard calibration procedures have in common: they are valid only under the assumption that the waves represent a single propagating mode within the calibration standard and the DUT. If this condition is not satisfied, a multimode calibration procedure must be introduced.

Returning to the TRL calibration procedure, it is useful to describe the general principles and implementation of the multiline TRL calibration before discussing the specific case of on-wafer multiline TRL. The TRL calibration procedure was originally introduced in [24] for calibration of dual six-port network analyzers, but is commonly used in conventional VNA calibrations. For calibration of two port VNA measurements, it is convenient to introduce the concept of error boxes that describe deviations of the VNA from ideal behavior. In this model, incident (outgoing) waves going in to (out of) the ideal VNA are entering (exiting) the error boxes at some fictitious reference planes. This approach is justified because the four port reflectometers of the network analyzer can be reduced to a cascade of two port equations [25]. For a two-port measurement, the error boxes take the form a two by two matrix. In turn, the calibration problem takes a form similar to Equations (2.48) and (2.64), where the fixture matrices are replaced by error boxes. In contrast to the fixture matrices, the error boxes do not in general satisfy the reciprocity requirement. The error boxes may be determined by solving a set of equations for set calibration standards, each of which is in the form of (2.55).

As originally conceived, three calibration standards were used in the TRL calibration. First, a “thru” standard was established by directly connecting ports 1 and 2 at the coaxial reference planes (the outer pair of reference planes in Fig. 2.5). Second, each port is terminated at the coaxial reference planes by a short circuit, open circuit or any impedance that has a load out of center of the Smith chart and is the same for both ports. The third standard is established by connecting a line of a known length between the coaxial reference planes. Note that this line has a different length than the thru line.

Early implementations of TRL faced a number of difficulties that were ultimately overcome by extending the technique by use of multiple, redundant lines. For instance, early implementations of TRL were band limited due to fact that the line length had to differ from $\lambda/2$, where λ is the wavelength of the source signal. For broadband

measurements, additional lines had to be introduced, but this approach introduced continuity problems at the boundaries of the frequency bands. Further, the approach did not take advantage of the fact that multiple lines provided redundant measurements that could potentially reduce measurement errors. These problems were ultimately solved by Bianco et al. [27] and Marks [26], who utilized multiple redundant line standards in the TRL calibration procedure, culminating in the technique we now know as multiline TRL. In multiline TRL, the calibration standards consist of set of transmission lines that differ only in length, the shortest of which serves as the thru standard, as well as reflection standards, which are assumed to be the same for both port connections. The procedure is based on estimation of the propagation constant of the transmission line standards at each measured frequency. Then the S-parameter correction coefficients are calculated using the accurate estimate of the propagation constant. The multiline TRL approach may be represented by an error box formulation as shown in Fig. 2.6.

Figure 2.6. **Two-port, eight-term error model.** The S parameters of the DUT are S_{ij} and the eight error terms are e_{ij} .

Importantly, the so called “switch terms” must be measured in addition to the calibration standards. The switch terms are specific to a given network analyzer, and account for differences between the forward and reverse match conditions. The switch terms can be measured only if all four wave parameters are accessible via the measurement instrument. Typically, the switch terms are measured simultaneously with the thru standard. The forward (Γ_{FW}) and reverse (Γ_R) switch terms are defined as

$$\Gamma_{FW} = \left. \frac{a_{2m}}{b_{2m}} \right|_{Source=Port1} ; \Gamma_R = \left. \frac{a_{1m}}{b_{1m}} \right|_{Source=Port2} . \quad (2.65)$$

Multiline TRL is in general done in two steps. In the first step, the propagation constant and line corrections are obtained. In the second step, the corrected lines are used to get the error box parameters. This is accomplished by analytically solving the eigenvalue problem following from the cascaded ports in Fig. 2.6. Several software packages are available for this calibration, including the NISTcal and STATISTICAL among other programs.

Note that while the S-parameters are defined relative to the characteristic impedance of the transmission line standards, Z_0 , multiline TRL obtains the propagation constant and the correction parameters without knowledge of the characteristic impedance. Once Z_0 is ultimately known, the correction coefficients can be transformed to any reference impedance. In addition, it is useful to know the length of the calibration lines or at minimum their relative length differences. This enables the selection of line pairs at each frequency that in turn avoids singularities in the calculation and improves the

accuracy of the propagation constant and error box parameters by averaging the results from the line pairs.

2.6.3 On-wafer calibration

Now we turn to on-wafer calibration procedures. Many nanoscale devices are incorporated into “on-chip” or “on-wafer” devices. Thus, we will introduce the basic concepts of on-wafer calibration and discuss some of the simpler error correction schemes. Our discussion in this chapter will be limited to the extension of multiline TRL to an on-wafer environment. In Chapter 4, on-wafer measurement instrumentation and other practical considerations are discussed and in Chapter 6, an example of a calibrated, on-wafer measurement of a nanowire device is given.

On-wafer waveguide structures are usually in the form of a microstripline or coplanar waveguide. These structures are contacted with a set of specially designed probes. During calibration, the probes are treated as part of the test fixture. The tips of the probe now define the position of the reference plane that we have up until now referred to as the “coaxial” reference plane. For the on-wafer multiline TRL calibration, the standards must have the same contact layout and geometry as the “fixture lines” of the DUTs. As in the multiline calibration approach described above, we once again obtain the propagation constant, the error boxes and the corrected lines and we use the error boxes to correct the S-parameters of the DUT. The error boxes include the properties of both the probes and the test platform, including the vector network analyzer. As long as the connecting transmission lines within the DUT have the same configuration as the calibration standards, one can translate the reference planes as described in Equation (2.60). Reference plane translation is often utilized in RF nanoelectronic devices to move the reference plane position as close as possible to the nanoscale building block(s) within the device.

2.7 Multimode calibration

A significant limiting factor of standard calibration procedures is that they require single-mode propagation at the reference planes. This may not be always the case: multimode propagation can easily occur when coupled or multiline waveguides are investigated and may occur in some nanoelectronic devices. Therefore, it is important to address the more complicated case of calibration when there are multiple modes propagating at the reference plans. The philosophy of multimode calibration follows basic multiport calibration techniques. Multimode calibration assumes that each mode propagates from its own effective port. Under this assumption the problem of multimode calibration is recast as a multiport calibration procedure where the number of physical ports is multiplied by the number of propagating modes. Instead of solving for propagation constants and error boxes at each port, one solves for unique propagation constants and error boxes corresponding to each propagating mode. The multimode TRL calibration technique was first introduced in Reference [29], but we

will follow the approach introduced in Reference [30]. The multimode TRL calibration can be divided in three main steps. As in the multiline TRL calibration, the first step focuses on determination of the propagation constants of all of the propagating modes based on measurements of the thru and line standards. In the second step the error box matrices \mathbf{T}_A , \mathbf{T}_B are partially determined. In the third step, a reflect measurement is used to reduce the number of unknowns in these matrices.

Here, we will describe the two-port device case, which can be extended to an arbitrary number of ports. We introduce the generalized reverse cascade matrix approach, which may simplify some problems in which symmetry is present. Such cases are not that common generally, but are present in some de-embedding cases that are discussed in following chapters. In a generalized scattering matrix of a multimode two-port device, all incident waves at port 1, incorporating power waves for N modes, are represented by an incident wave vector \mathbf{A}_1 . Similarly, all reflected waves at port 1 are represented by the vector \mathbf{B}_1 . The vectors \mathbf{A}_2 and \mathbf{B}_2 represent the incident and reflected waves at port 2 of the generalized two-port device. The vectors are defined:

$$\mathbf{A}_1 = \begin{bmatrix} a_1 \\ \vdots \\ a_N \end{bmatrix} \quad ; \quad \mathbf{A}_2 = \begin{bmatrix} a_{N+1} \\ \vdots \\ a_{2N} \end{bmatrix} \quad , \quad (2.66a)$$

and

$$\mathbf{B}_1 = \begin{bmatrix} b_1 \\ \vdots \\ b_N \end{bmatrix} \quad ; \quad \mathbf{B}_2 = \begin{bmatrix} b_{N+1} \\ \vdots \\ b_{2N} \end{bmatrix} \quad . \quad (2.66b)$$

This definition enables a scattering matrix definition that includes transmission between N modes at port 1 and N modes at port 2. Thus, this definition also includes the mixing of the modes from different ports. Further, it can also incorporate evanescent modes.

The generalized scattering matrices are related to the generalized incident and reflected wave vectors by

$$\begin{bmatrix} \mathbf{B}_1 \\ \mathbf{B}_2 \end{bmatrix} = \begin{bmatrix} \mathbf{S}_{11} & \mathbf{S}_{12} \\ \mathbf{S}_{21} & \mathbf{S}_{22} \end{bmatrix} \begin{bmatrix} \mathbf{A}_1 \\ \mathbf{A}_2 \end{bmatrix} \quad , \quad (2.67)$$

where \mathbf{S}_{ij} are $N \times N$ submatrices. In a similar way one can introduce the generalized left to right cascade (transmission) matrix

$$\begin{bmatrix} \mathbf{B}_1 \\ \mathbf{A}_2 \end{bmatrix} = \begin{bmatrix} \mathbf{T}_{11} & \mathbf{T}_{12} \\ \mathbf{T}_{21} & \mathbf{T}_{22} \end{bmatrix} \begin{bmatrix} \mathbf{A}_1 \\ \mathbf{B}_2 \end{bmatrix} \quad . \quad (2.68)$$

The conversion between from the generalized scattering matrix to the generalized cascade matrix is similar to (2.61) with scalar S parameters replaced by \mathbf{S} submatrices. This conversion is possible only if \mathbf{S}_{21} is nonsingular. One can also introduce the left-to

right reverse cascade matrix (or connected right to left). Simple arithmetic manipulation shows that

$$\begin{bmatrix} \mathbf{B}_2 \\ \mathbf{A}_2 \end{bmatrix} = [\bar{\mathbf{T}}] \begin{bmatrix} \mathbf{A}_1 \\ \mathbf{B}_1 \end{bmatrix}, \quad (2.69)$$

with the reverse cascade matrix

$$\bar{\mathbf{T}} = \mathbf{P}\mathbf{T}^{-1}\mathbf{P}; \mathbf{P} = \begin{bmatrix} \mathbf{0} & \mathbf{I} \\ \mathbf{I} & \mathbf{0} \end{bmatrix}. \quad (2.70)$$

This matrix represents the mirrored (connected right-to-left) version of the original left-to-right matrix. \mathbf{P} is a $2N \times 2N$ permutation matrix with \mathbf{I} a $N \times N$ unity matrix.

In this notation the calibrated two port network analyzer measures the scattering parameter matrix \mathbf{M} :

$$\mathbf{M} = \mathbf{T}^A \mathbf{T}^{DUT} \bar{\mathbf{T}}^B, \quad (2.71)$$

where \mathbf{T}^{DUT} is the cascade matrix of the DUT and the matrices \mathbf{T}^A and \mathbf{T}^B represent the error boxes. With these definitions in place, the multimode calibration procedure is analogous to the single-mode case. Specifically, similar calibration standards are measured. It is assumed though that these standards can support multiple quasi-TEM propagating modes corresponding to the modes supported by the DUT. The complex propagation constants of the multiple modes, as well as the matrices \mathbf{T}^A and \mathbf{T}^B are determined in steps similar to those in the single-mode case. Additional details of the procedure can be found in References [29] and [30].

2.8 Calibration of a scanning microwave microscope and other one-port systems

We conclude this chapter with a specific calibration approach that is important for local, near-field probes such as near-field scanning microwave microscopes (NSMMs). The calibration of the near-field probing measurements is particularly challenging because the condition of single-mode propagation is not satisfied for near fields. Fortunately, this problem can be avoided for most NSMM measurements if they are done in a single-port configuration, i.e. if the microwave signal path in the NSMM can be represented as a one-port network. This is true for the vast majority of existing NSMMs that are based on atomic force and scanning tunneling microscope systems.

For single-port NSMMs the measurand is the complex reflection coefficient S_{11m} . The near-field interaction is localized at the tip and thus will be included in the de-embedded properties of the measured DUT. The effects of near-field interaction cannot be removed by calibration. Quantifying and understanding this interaction must be done by analyzing and interpreting the calibrated measurement results.

In the single-port case the signal flow graph shown in Fig. 2.6 is simplified to the graph shown in Fig. 2.7. The terms in Fig. 2.7 are defined as follows: e_{00} is directivity, the product $e_{10}e_{01}$ is tracking and e_{11} is the port match [31]. Using the signal flow graph rules the relation between the measured and actual reflection coefficients is

$$S_{11m} = e_{00} + \frac{e_{01}e_{10}\Gamma_L}{1-e_{11}\Gamma_L} \quad , \quad (2.72)$$

where Γ_L is the de-embedded reflection coefficient of the DUT, as shown in Fig. 2.7. From this equation, it follows that to calibrate any one port measurement, including one obtained with an NSMM, it is necessary to solve a system of equations for three complex values, which requires no fewer than three measurements of calibration standards. Specific approaches to NSMM calibration will be discussed in Chapter 7.

Figure 2.7. Error model for an NSMM and other one port measurements. This model includes three error terms: e_{00} is directivity, the product $e_{10}e_{01}$ is tracking and e_{11} is the port match.

References

- [1] P. A. Rizzi, *Microwave Engineering Passive Circuits* (Prentice Hall, 1988)
- [2] R. F. Harrington, *Time-harmonic electromagnetic fields* (Wiley, 2001).
- [3] O. Keller, *Quantum theory of near field electrodynamics* (Springer, 2011).
- [4] J. D. Jackson, *Classical Electrodynamics* (John Wiley 1975).
- [5] J. A. Stratton, *Electromagnetic Theory* (McGraw Hill, 1941).
- [6] H. Hertz, "Die Kräfte electrischer Schwingungen, behandelt nach Maxwellschen Theorie, *Ann. Physik*, **36** (1888) pp.1-22
- [7] D. M. Kerns, "Plane-wave scattering matrix theory of antennas and antenna-antenna interactions," *National Bureau of Standards Monograph 162* (1981).
- [8] D. M. Pozar, *Microwave engineering* (Wiley, 2004).
- [9] K.C. Gupta, R. Garg, I. Bahl, P. Bhartia, *Microstrip lines and slotlines* (Artech House, 1996).
- [10] R.E. Collin *Foundations of Microwave Engineering* (McGraw Hill, 1992).
- [11] L. D. Landau and E.M. Lifshitz, *Classical Theory of Fields* (Pergamon Press, 1962).
- [12] J. C. Slater, "Microwave Electronics," *Reviews of Modern Physics* **18** (1946) pp. 441-512.
- [13] O. Heaviside, *Electromagnetic Theory: complete and unabridged edition v.1 no. 2 and v.3*, (Dover , 1950).
- [14] A. Sommerfeld, *Electrodynamics*, (Academic Press, 1952). R. J. Collier, *Transmission lines: equivalent circuits, electromagnetic theory, and photons* (Cambridge, 2013),
- [15] F. Olyslager, *Electromagnetic waveguides and transmission lines* (Oxford, 1999).
- [16] R. A. Chipman, *Theory and Problems of Transmission Lines* (McGraw-Hill, 1968).
- [17] G. Mathaei, L. Young and E.M.T. Jones, *Microwave Filters, Impedance-Matching Networks, and Coupling Structures* (Artech House, 1980).
- [18] K. Kurokawa, "Power Waves and the Scattering Matrix", *IEEE Transactions on Microwave Theory & Techniques*, **13** (1965) pp. 194-202.
- [19] S. J. Mason, "Feedback theory - some properties of signal flow graphs," *Proceedings of the IRE* **41** (1963) pp. 1144-1156. F. Caspers, "RF Engineering basic concepts: S-parameters," arXiv:1201.2346 [physics.acc-ph].

- [20] S. J. Mason, "Feedback theory - further properties of signal flow graphs," *Proceedings of the IRE* **44** (1956) pp. 920-926.
- [21] "S-Parameter Design," *Agilent Application Note 154* (Agilent Technologies, 2006).
- [22] "Vector network analyzer primer" *Anritsu Application note 11410-00387* (Anritsu Company, 2009).
- [23] "Measuring balanced components with Vector Network Analyzer ZVB" *Rhode & Schwartz Application note 1EZ53_0E* (Rhode & Schwartz, 2004).
- [24] G. F. Engen and C. A. Hoer, "Thru-Reflect-Line: an improved technique for calibrating a dual six-port automatic network analyzer," *IEEE Transactions on Microwave Theory and Techniques* **27** (1979) pp. 987-993.
- [25] H.-J. Eul and B. Schiek, "A general theory and new calibration procedures for network analyzer self-calibration," *IEEE Transactions on Microwave Theory and Techniques* **39** (1991) p. 724-731.
- [26] R. Marks, "A multiline method of network analyzer calibration," *IEEE Transactions on Microwave Theory and Techniques* **39** (1991) p. 1205-1215.
- [27] B. Bianco, M. Parodi, S. Ridella, and F. Selvaggi, "Launcher and microstrip characterization," *IEEE Transactions on Instrumentation and Measurement* **25** (1976) pp. 320-323.
- [28] C. Sequinot, P. Kennis, J-F. Legier, F. Huret, E. Paleczny, and L. Hayden, "Multimode TRL-New concept in microwave measurements: Theory and experimental verification," *IEEE Transactions on Microwave Theory and Techniques* **46** (1998) pp. 536.
- [29] M. Wojnowski, V. Issakov, G. Sommer, R. Weige, "Multimode TRL calibration technique for characterization of differential devices," *IEEE Transactions on Microwave Theory and Techniques* **60**, (2012) pp.2220.
- [30] "De-embedding and embedding S-parameter networks using a vector network analyzer," Agilent Application Note 1364-1 (Agilent/Keysight Technologies, 2004)

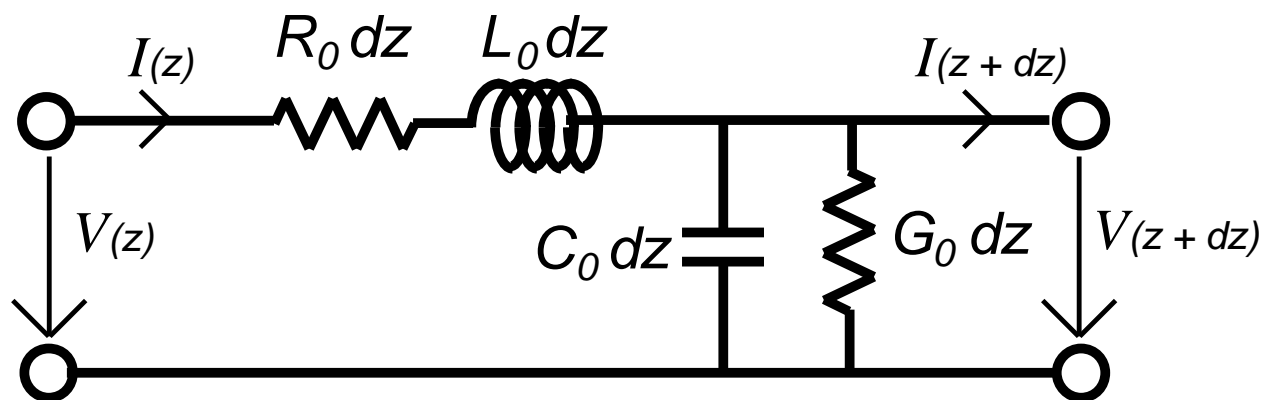


FIGURE 2-1.

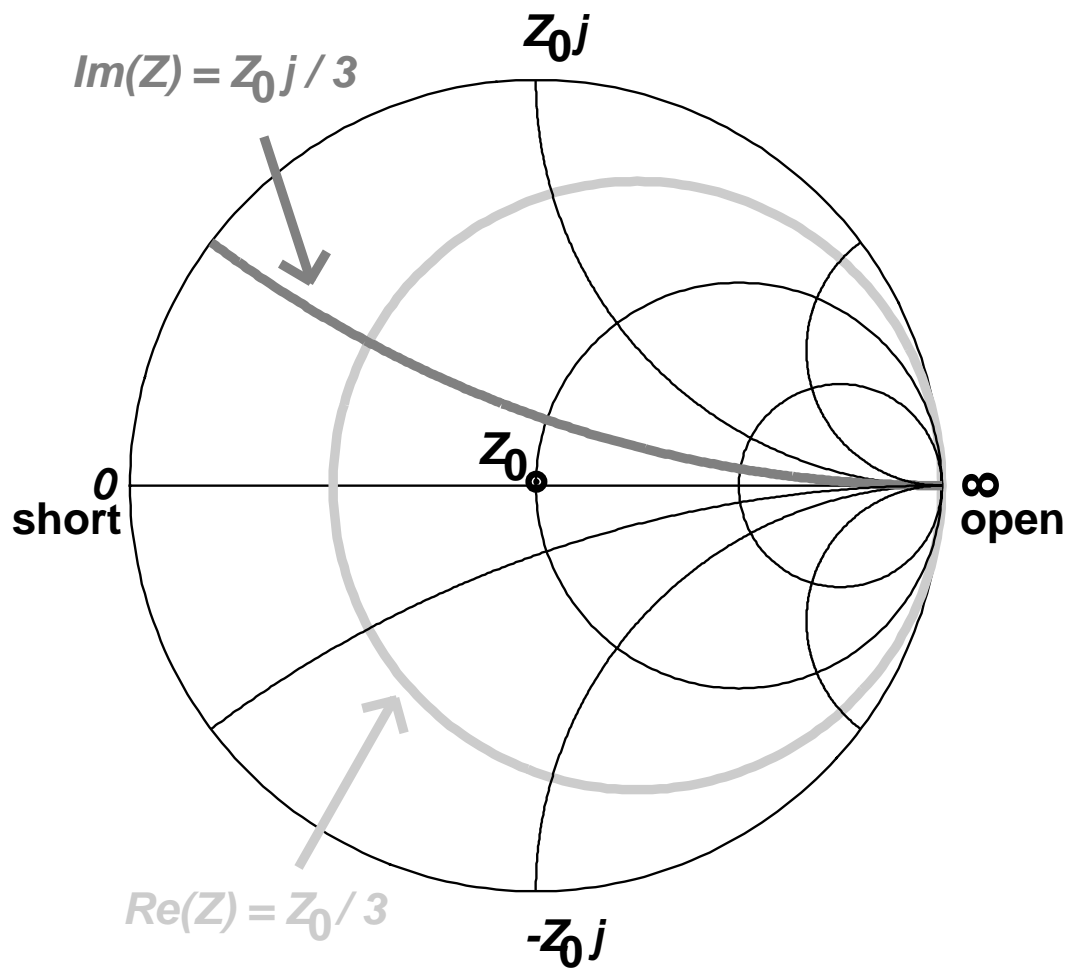


FIGURE 2-2.

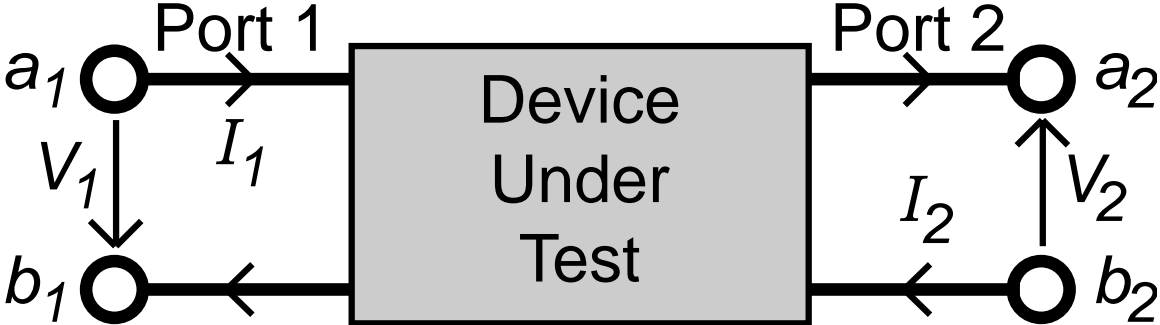


FIGURE 2-3.

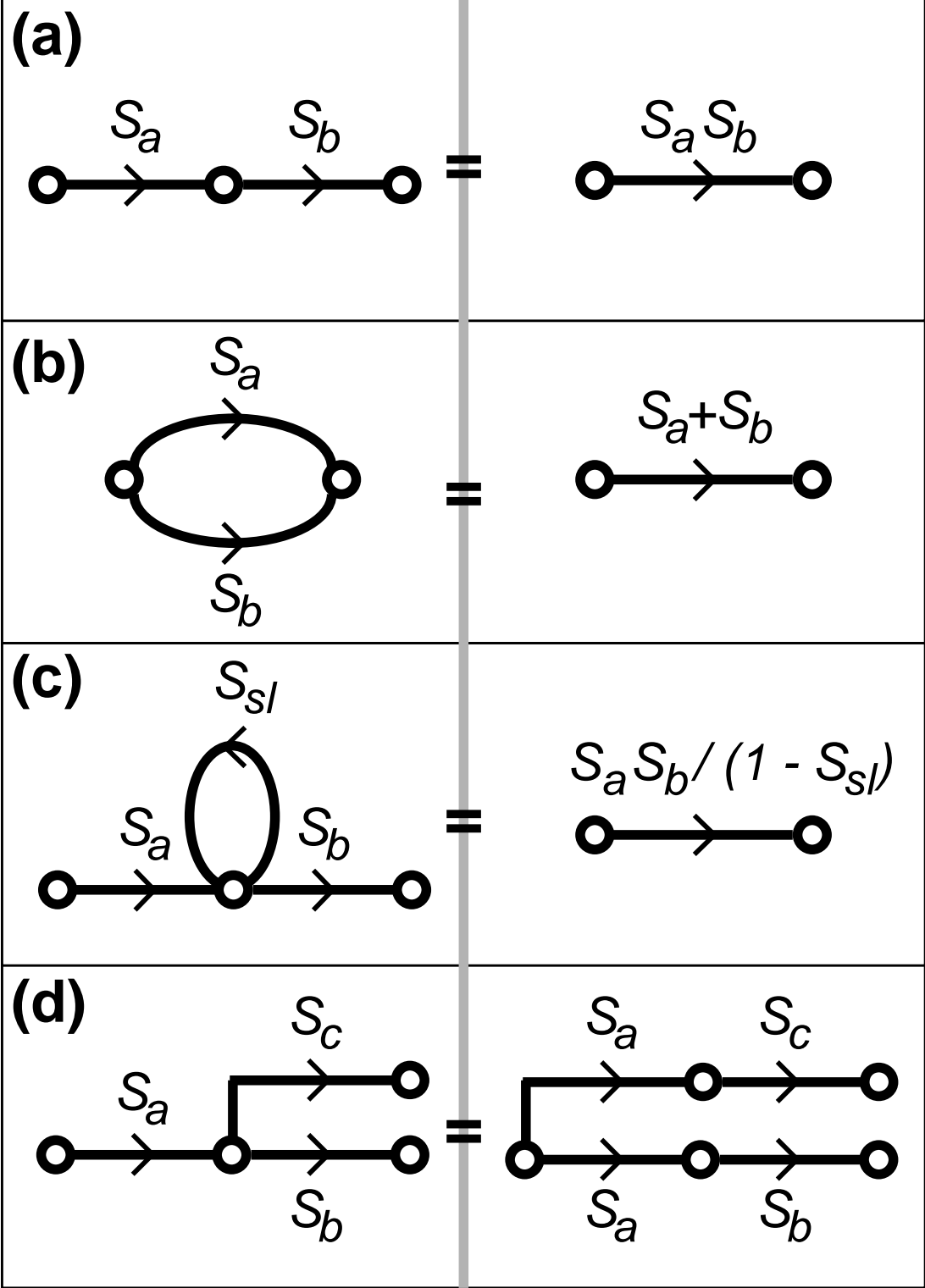


FIGURE 2-4.

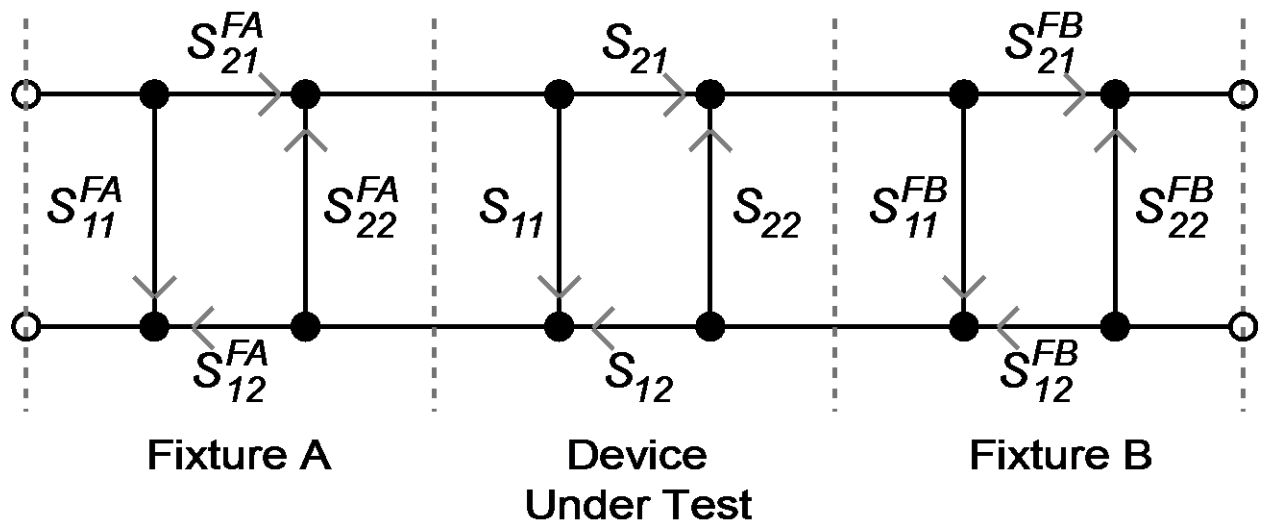


FIGURE 2-5.

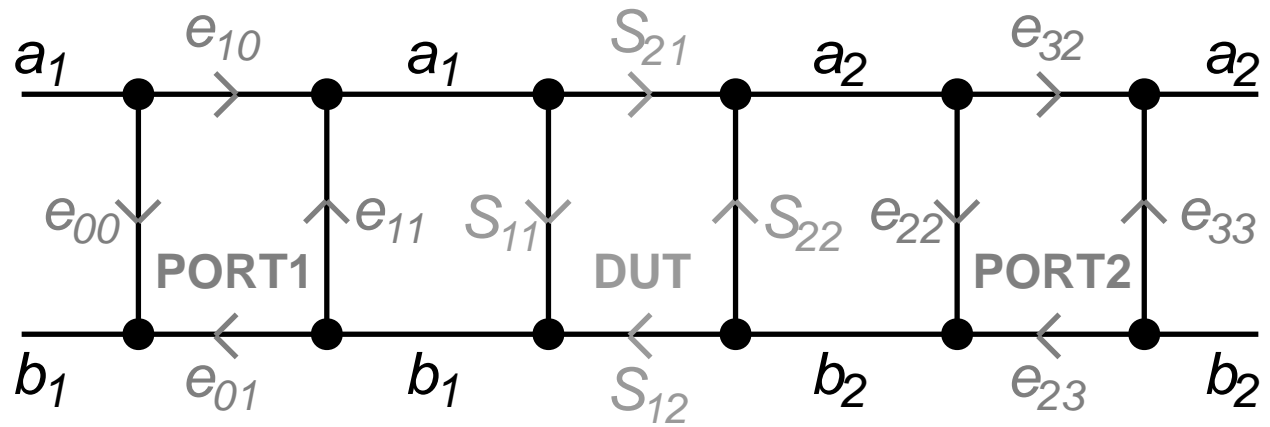


FIGURE 2-6.

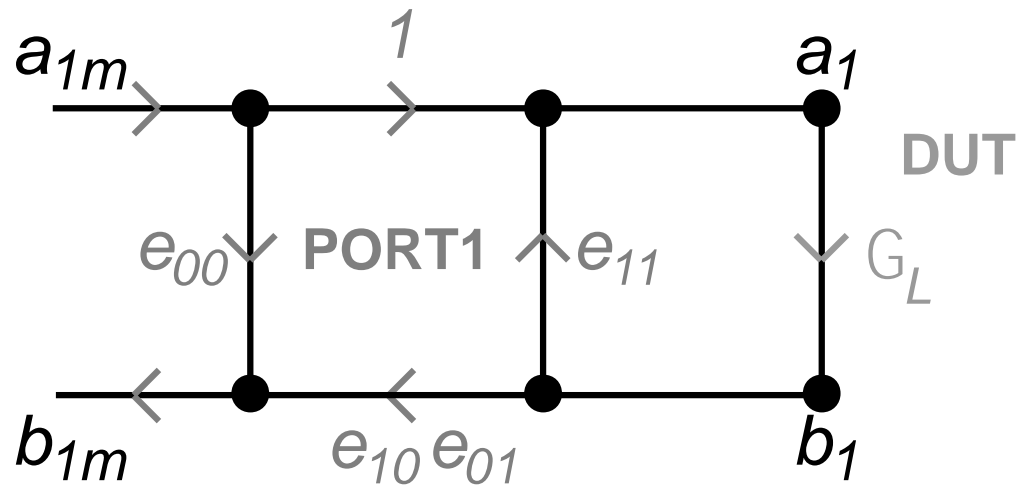


FIGURE 2-7.